Supplementary Materials

Fomes fomentarius as a bio-template for heteroatom-doped carbon fibers for symmetrical supercapacitors

Daria Chernysheva [1,*], Maksim Konstantinov [1], Ekaterina Sidash [1], Tatiana Baranova [1], Victor Klushin [1], Denis Tokarev [1], Veronica Andreeva [1], Evgeny Kolesnikov [2], Vasily Kaichev [3], Mikhail Gorshenkov [2], and Nina Smirnova [1,*]

[1]Platov South-Russian State Polytechnic University (NPI), Novocherkassk, Russia
[2]National University of Science and Technology MISiS, Moscow, Russia
[3]Boreskov Institute of Catalysis, Novosibirsk, Russia
*Correspondence: da.leontyva@mail.ru; smirnova_nv@mail.ru

Structural measurements

The specific surface areas (SSAs) of the obtained materials were determined by using a TOP-200 surface area and porosity analyzer (Altamira instruments, USA) and calculated from N_2 adsorption/desorption isotherms according to the Brunauer–Emmett–Teller method. The samples were degassed at 100 °C under vacuum for 24 h prior to the N_2 adsorption measurements. The measurements were carried out at -196,15 °C. The pore size distributions were calculated from the desorption branches of the isotherms by using the Barrett–Joyner–Halenda (BJH) model and the density functional theory (DFT) model.

Electrochemical measurements

Electrochemical studies were carried out at room temperature in a three-electrode cell using a P-45X potentiostat/galvanostat (Elins). Cyclic voltammetry (CV) was carried out in the potential range from -1 to -0.1 V at different potential sweep rates (5, 10, 20, 50, and 100 mV/s) using a 6 M aqueous solution of KOH as the electrolyte. Galvanostatic studies in the charge/discharge mode at different current densities (0.2, 0.5, 1, 2, 5, and 10 A/g), as well as the study of stability during long-term cycling in the charge/discharge mode, were carried out in the same potential range.

A multichannel potentiostat/galvanostat (Elins) was used to conduct studies on symmetrical two-electrode coin cells (CR2025) with an aqueous electrolyte (6 M KOH) and polypropylene membrane (PORP A1) as a separator. The CV of the coin cells was carried out in the potential range from 0 to 1 V at different scan rates. Galvanostatic studies in charge/discharge mode at different current densities (0.005, 0.002, 0.01, 0.02, 0.05, 0.1, and 0.2 A/g) and long-term charge/discharge cycling were performed in the same range of potentials.

The energy density and power density were calculated according to the equations S1–S3. The specific capacitance of the coin cell considering the total mass of active materials on both electrodes is [51]:

$$C_{s\,(cell)} = \frac{2 \cdot I \cdot \Delta t}{M \cdot \Delta V} \quad \text{(S1)},$$

where $C_{s(cell)}$ is the specific capacitance (F/g), I is the discharging current (A), Δt is the discharge time (s), M is the total mass of the carbon materials on both electrodes (g), and ΔV is the potential window (V).

The energy density and power density were calculated from the discharge curves [51]:

$$E = \frac{1}{2 \cdot 3.6} \cdot C_{s(cell)} \cdot (\Delta V)^2 \quad \text{(S2)}$$

$$P = 3600 \cdot \frac{E}{\Delta t} \quad \text{(S3)}$$

where E is the energy density (Wh/kg), P is the power density (W/kg), $C_{s(cell)}$ is the specific capacitance of the coin cell (F/g), ΔV is the potential window (V), and Δt is the discharge time (s).

The Ragone plot for the symmetric coin cell, which shows the relationship between the energy and power densities, is shown in Figure S1.

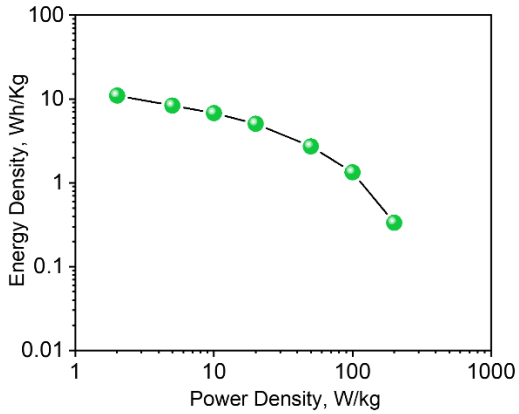


Figure S1. Ragone plot for a symmetric coin cell with HT-P-ChP-T as the electrode material.

Table S1. Comparing the electrochemical performances of carbon material from this work with other carbon electrode materials.

Carbon precursor	Sample	SSA, $m^2 g^{-1}$	Electrolyte	Cell Type	Mass Loading of Electrode Material	Max. Specific Capacity, $F g^{-1}$	Cycling Stability	Ref.
Fomes fomentarius	HT-P-ChP-T	1491	6 M KOH	3 el.	1.4	220 (at 0.2 A g^{-1})	92% after 25000 cycles at 10 A g^{-1}	This study
				2 el.	10±1	158 (at 2 mA g^{-1})	-	
Auricularia fungus	P-HT-A	80	6 M KOH	3 el.	-	196 (at 5 mV s^{-1})	99% after 1000 cycles	[35]
Bamboo fungus	NHPC-800	1708	2 M KOH	3 el.	2	228 (at 0.5 A g^{-1})	100% after 10000 cycles at 40 A g^{-1}	[32]
				2 el.		30.6 (at 0.5 A g^{-1})	100% after 10000 cycles at 10 A g^{-1}	
Fungi strains of X. ylaria	N-S-FHCF	789.52	6 M KOH	3 el.	5.0-6.0	216 (at 1 A g^{-1})	83.4% after 3000 cycles at 1 A g^{-1}	[33]
Aniline modified fungus	N–AC	2339	6 M KOH	3 el.	-	218 (at 0.1 A g^{-1})	100% after 5000 cycles at different current densities	[34]
Pleurotus ostreatus stipe	PCK	2149	1 M Na_2SO_4	3 el.	-	77 (at 1 A g^{-1})	-	[36]
				2 el.	-	86 (at 1 A g^{-1})	98% after 10000 cycles at 5 A g^{-1}	
Sugar beet pulp	SC-Zn-700	950	6 M KOH	3 el.	2.0-3.0	263 (at 0.5 A g^{-1})	-	[71]
				2 el.	2.0-3.0	52 (at 0.5 A g^{-1})	83% after 10000 cycles at a scan rate of 200 mV s^{-1}	
Soybean	ANPC-3	1749	6 M KOH	3 el.	-	243 (at 0.5 A g^{-1})	-	[52]
			0.5 M Na_2SO_4	2 el.	-	116.5 (at 0.5 A g^{-1})	96.5% after 5000 cycles at 1 A g^{-1}	
Eucommia ulmoides Oliver wood	EUOAC4	1456.69	1M H_2SO_4	3 el.	2	158 (at 0.2 A g^{-1})	93% after 5000 cycles at 1 A g^{-1}	[69]
Corn starch	PC/500/1/4:1	1167	6 M KOH	3 el.	-	162 (at 0.625 A g^{-1})	93% after 5000 cycles at 0.625 A g^{-1}	[48]
Cotton pulp	Carbonized at 1000 °C	346.11	5 M KCl	3 el.	-	107 (at 1 A g^{-1})	90% after 2000 cycles at 1 A g^{-1}	[70]
Poplar wood	NPAC	529.4	6 M KOH	3 el.	-	181.3	-	[64]

						(at 1 A g^{-1})		
Sewage sludge	SWC-900	480.3	1 M Na_2SO_4	3 el.	-	113.9 (at 5 mV s^{-1})	93% after 10000 cycles	[56]
Polymer-based carbon spheres	P800	595	1 M H_2SO_4	3 el.	2-4	132 (at 0.1 A g^{-1})	-	[60]
				2 el.	2-4	157 (at 0.05 A g^{-1})	-	

References

32. Zou, Z.; Lei, Y.; Li, Y.; Zhang, Y.; Xiao, W. Nitrogen-Doped Hierarchical Meso/Microporous Carbon from Bamboo Fungus for Symmetric Supercapacitor Applications. Molecules 2019, 24, 3677.
33. Lei, J.; Guo, Q.; Yao, W.; Duan, T.; Chen, P.; Zhu, W. Bioconcentration of organic dyes via fungal hyphae and their derived carbon fibers for supercapacitors. Journal of Materials Chemistry A 2018, 6, 10710-10717, doi:10.1039/C8TA02655F.
34. Wang, K.; Xu, M.; Wang, X.; Gu, Z.; Fan, Q.H.; Gibbons, W.; Croat, J. Porous carbon derived from aniline-modified fungus for symmetrical supercapacitor electrodes. RSC Advances 2017, 7, 8236-8240, doi:10.1039/C6RA27600H.
35. Zhu, H.; Wang, X.; Yang, F.; Yang, X. Promising Carbons for Supercapacitors Derived from Fungi. Advanced Materials 2011, 23, 2745-2748, doi:https://doi.org/10.1002/adma.201100901.
36. Li, X.; Liang, P.; Zhang, J.; Liu, B. Electrochemical performance of Pleurotus ostreatus-derived carbon prepared by different methods as electrode in supercapacitor. Materials Chemistry and Physics 2022, 278, 125623, doi:https://doi.org/10.1016/j.matchemphys.2021.125623.
48. Pang, L.; Zou, B.; Han, X.; Cao, L.; Wang, W.; Guo, Y. One-step synthesis of high-performance porous carbon from corn starch for supercapacitor. Materials Letters 2016, 184, 88-91, doi:https://doi.org/10.1016/j.matlet.2016.07.147.
51. Chernysheva, D.; Sidash, E.; Konstantinov, M.; Klushin, V.; Tokarev, D.; Andreeva, V.; Kolesnikov, E.; Kaichev, V.; Smirnova, N.; Ananikov, V.P. "Liquid-to-solid" conversion of biomass wastes enhanced by nitrogen doping for the preparation of high-value-added carbon materials for energy storage with superior characteristics. ChemSusChem 2023, n/a, doi:https://doi.org/10.1002/cssc.202202065.
52. Lin, G.; Ma, R.; Zhou, Y.; Liu, Q.; Dong, X.; Wang, J. KOH activation of biomass-derived nitrogen-doped carbons for supercapacitor and electrocatalytic oxygen reduction. Electrochimica Acta 2018, 261, 49-57, doi:https://doi.org/10.1016/j.electacta.2017.12.107.
56. Li, X.; Hao, T.; Tang, Y.; Chen, G. A "Seawater-in-Sludge" approach for capacitive biochar production via the alkaline and alkaline earth metals activation. Frontiers of Environmental Science & Engineering 2020, 15, 3, doi:10.1007/s11783-020-1295-0.
60. Huang, C.; Puziy, A.M.; Poddubnaya, O.I.; Hulicova-Jurcakova, D.; Sobiesiak, M.; Gawdzik, B. Phosphorus, nitrogen and oxygen co-doped polymer-based core-shell carbon sphere for high-performance hybrid supercapacitors. Electrochimica Acta 2018, 270, 339-351, doi:https://doi.org/10.1016/j.electacta.2018.02.115.
64. Li, K.; Wang, B.; Bolatibieke, D.; Nan, D.-h.; Lu, Q. Pyrolysis of Biomass Impregnated With Ammonium Dihydrogen Phosphate for Polygeneration of Phenol and Supercapacitor Electrode Material. Front. Chem. 2020, 8, 436, doi:10.3389/fchem.2020.00436.
69. Sun, G.; Qiu, L.; Zhu, M.; Kang, K.; Guo, X. Activated carbons prepared by hydrothermal pretreatment and chemical activation of Eucommia ulmoides wood for supercapacitors application. Industrial Crops and Products 2018, 125, 41-49, doi:https://doi.org/10.1016/j.indcrop.2018.08.082.
70. Jiang, L.; Nelson, G.W.; Han, S.O.; Kim, H.; Sim, I.N.; Foord, J.S. Natural Cellulose Materials for Supercapacitors. Electrochimica Acta 2016, 192, 251-258, doi:https://doi.org/10.1016/j.electacta.2015.12.138.
71. Gür, E.; Semerci, T.G.; Semerci, F. Sugar beet pulp derived oxygen-rich porous carbons for supercapacitor applications. Journal of Energy Storage 2022, 51, 104363, doi:https://doi.org/10.1016/j.est.2022.104363.